Environmental Science & Technology

Article

pubs.acs.org/est

Temporal Trends in Atmospheric $PM_{2.5}$, PM_{10}, Elemental Carbon, Organic Carbon, Water-Soluble Organic Carbon, and Optical Properties: Impact of Biomass Burning Emissions in The Indo-Gangetic Plain

Kirpa Ram,[†,∥] M. M. Sarin,*[,†] and S. N. Tripathi[‡]

[†]Physical Research Laboratory, Ahmedabad, India

[‡]Department of Civil Engineering and Center for Environmental Science and Engineering, Indian Institute of Technology, Kanpur, India

Supporting Information

ABSTRACT: The first simultaneous measurements and analytical data on atmospheric concentrations of $PM_{2.5}$, PM_{10}, inorganic constituents, carbonaceous species, and their optical properties (aerosol optical depth, AOD; absorption coefficient, b_{abs}; mass absorption efficiency, σ_{abs}; and single scattering albedo, SSA) from an urban site (Kanpur) in the Indo-Gangetic Plain are reported here. Significantly high aerosol mass concentration (>100 μg m^{-3}) and AOD (> 0.3) are seen as a characteristic feature throughout the sampling period, from October 2008 to April 2009. The temporal variability in the mass fractions of carbonaceous species (EC, OC, and WSOC) is pronounced during October–January when emissions from biomass burning are dominant and OC is a major constituent (~30%) of $PM_{2.5}$ mass. The WSOC/OC ratio varies from 0.21 to 0.65, suggesting significant contribution from secondary organic aerosols (SOAs). The mass fraction of SO_4^{2-} in $PM_{2.5}$ (Av: 12.5%) exceeds that of NO_3^- and NH_4^+. Aerosol absorption coefficient (@ 678 nm) decreases from 90 Mm^{-1} (in December) to 20 Mm^{-1} (in April), and a linear regression analysis of the data for b_{abs} and EC (n = 54) provides a measure of the mass absorption efficiency of EC (9.6 m^2 g^{-1}). In contrast, scattering coefficient (@ 678 nm) increases from 98 Mm^{-1} (in January) to 1056 Mm^{-1} (in April) and an average mass scattering efficiency of 3.0 ± 0.9 m^2 g^{-1} is obtained for PM_{10} samples. The highest b_{scat} was associated with the dust storm event (April 17, 2009) over northern Iraq, eastern Syria, and southern Turkey; thus, resulting in high SSA (0.93 ± 0.02) during March–April compared to 0.82 ± 0.04 in October–February. These results have implications to large temporal variability in the atmospheric radiative forcing due to aerosols over northern India.

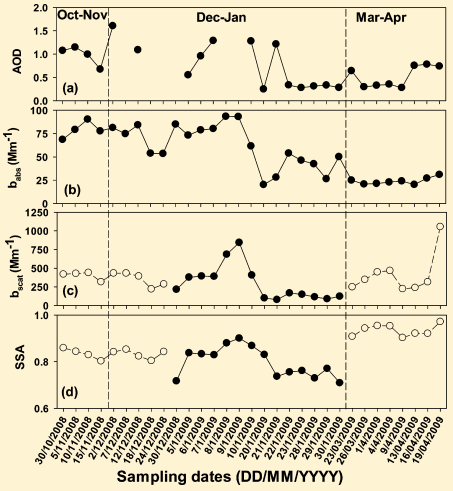

1. INTRODUCTION

In the present-day scenario of growing anthropogenic activities associated with emissions from fossil fuel, biomass burning, land use changes, and industrial development have led to rapid increase in the atmospheric concentrations of carbonaceous species in south and southeast Asia.[1−3] In this context, it is most relevant to study the aerosol characteristics (chemical, physical, and optical) from the Indo-Gangetic Plain (IGP). A large stretch of the IGP is influenced by emissions from post-harvest agricultural-waste burning, fossil-fuel combustion (vehicular, industrial, and thermal power plants), and a number of minor sources (e.g., brick kilns and textile mills).[4−7] The long-range transport of mineral dust originating from Iran, Afghanistan, Pakistan, and the Thar Desert (western India) imparts significant variability to the aerosol composition during summer months (March–June).[8−10] Furthermore, mixing of carbonaceous species with anthropogenic inorganic constituents has led to degradation of air quality, visibility impairment, and atmospheric brown cloud formation during the wintertime (December–February).[11−13] The transport and occurrence of pollutants over the Himalayan region, and their impact on monsoon circulation and rainfall pattern over India have been a subject of immense debate.[14,15]

It is, thus, essential to document spatial and temporal variability in the chemical composition and optical properties of ambient aerosols through ground-based measurements from northern India. This manuscript presents simultaneous measurements of $PM_{2.5}$, PM_{10}, organic carbon (OC), elemental carbon (EC), water-soluble OC (WSOC), inorganic constituents, and aerosol optical properties (aerosol optical depth, AOD; single scattering albedo, SSA; absorption and scattering

Received: August 16, 2011
Revised: December 5, 2011
Accepted: December 12, 2011
Published: December 12, 2011

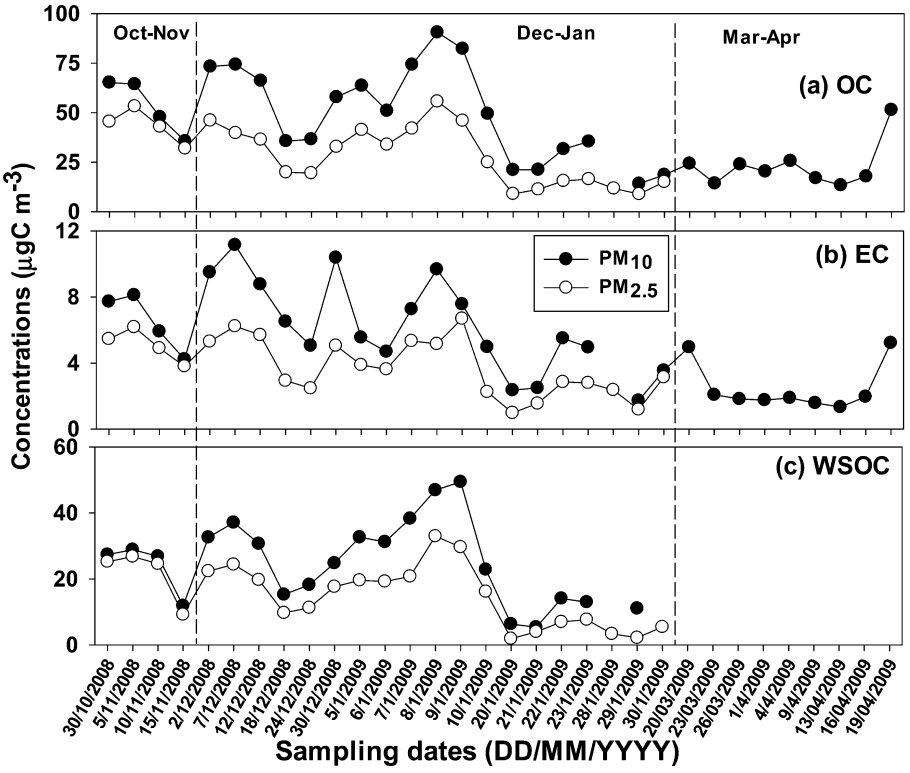

Figure 1. Temporal variability in the mass concentrations of (a) OC, (b) EC, and (c) WSOC in $PM_{2.5}$ and PM_{10} from an urban site (Kanpur) in the Indo-Gangetic Plain during the sampling period (October 2008 to April 2009).

coefficients, b_{abs} and b_{scat}; mass absorption and scattering efficiencies of EC and PM_{10}, σ_{abs} and σ_{PM10}, respectively) carried out over a period of six months (October 2008–April 2009) from an urban site (Kanpur) located in the center of the Indo-Gangetic Plain.

2. METHODOLOGY

2.1. Sampling Location and Aerosol Collection. The sampling site, Kanpur (26.5° N, 80.3° E) representing an urban environment, is ideally located in the Indo-Gangetic Plain in order to study the aerosol composition influenced by the upwind biomass-burning emissions and fossil-fuel combustion sources. A vast expanse of IGP experiences severe fog-haze weather conditions during the wintertime (December–February). Ambient aerosols, $PM_{2.5}$ and PM_{10} (particulate matter less than 2.5 and 10 μm aerodynamic diameter, respectively), were collected on precombusted quartz filters (Tissuquartz, 20 × 25 cm^2, Pall Life Sciences, USA) by simultaneously operating two high-volume samplers (Thermo Anderson, USA) at a flow rate of 1.1 ± 0.1 m^3 min^{-1}. Samplers were set up at ~15 m above ground level on the terrace of the Environmental Engineering Laboratory at the Indian Institute of Technology campus. Overall, one pair of $PM_{2.5}$ and PM_{10} was collected every fifth day during the sampling period from October 2008 to April 2009 (except January), and each sample was integrated for 6–8 h in order to filter ~500–600 m^3 of ambient air.

The concentrations of OC and EC were measured on an EC-OC analyzer (Sunset Laboratory, USA) using the thermo-optical transmittance (TOT) protocol. The correction for carbonate carbon (CC) was achieved by integrating the evolved CO_2 between 615 and 870 °C on the thermograph.[10] This CC peak was ascertained by exposing the filter aliquot to 6 M HCl fumes in a desiccator for 6–8 h. The analytical details for the measurement of OC and EC have been described in our earlier publications.[5,14,15] The concentration of water-soluble organic carbon was measured on a total organic carbon (TOC) analyzer (Shimadzu, model TOC-5000A) and inorganic constituents were measured by ion chromatograph (Dionex-500).[9,10,14] Simultaneously, several blank filters were analyzed (one blank with every set of 10 samples) in order to obtain their inherent concentrations on the filter. All the reported concentrations of measured chemical species in the present study have been corrected for their respective blank concentrations in the filters. The detection limit for OC (estimated as three times the standard deviation of blank signal of 1.5 ± 0.4 μgC cm^{-2} for $n = 6$) and EC (estimated using 0.2 μgC cm^{-2} as minimum detection capability of the instrument) are 0.8 and 0.15 μgC m^{-3}, respectively, for an average air volume of ~600 m^3. The contribution of OC and EC from blank filters is <2 and 4% of their respective average concentrations in aerosol samples. The reproducibility, based on replicate analyses, is ~3% for K^+, Ca^{2+}, Cl^-, SO_4^{2-}, and NO_3^- and ~6% for NH_4^+.

2.2. Aerosol Optical Properties. Aerosol optical properties, absorption and scattering coefficients (b_{abs} and b_{scat} at 678 and 781 nm, respectively), mass absorption efficiency (σ_{abs}), and mass scattering efficiency (MSE), were measured using a set of optical instruments. The absorption coefficient (b_{abs}) was measured, simultaneously with EC and OC mass concentrations, based on transmittance of the 678-nm laser source used in the EC-OC analyzer.[16] The σ_{abs} was then calculated by dividing absorption coefficient with EC mass concentration (i.e., $\sigma_{abs} = b_{abs}/EC$); the uncertainty is better than 20% for b_{abs} and 30% for σ_{abs}.[16]

dx.doi.org/10.1021/es202857w | Environ. Sci. Technol. 2012, 46, 686–695

Table 1. Average Mass Concentrations (in $\mu g\ m^{-3}$) of OC, EC, and WSOC ($\pm 1\sigma$) and Inorganic Species, along with OC/EC and WSOC/OC Ratios, at Kanpur during Different Time Periods

	Oct−Nov		Dec−Feb		Mar−Apr
	$PM_{2.5}$ (n = 4)	PM_{10} (n = 4)	$PM_{2.5}$ (n = 19)	PM_{10} (n = 18)	PM_{10} (n = 9)
mass	189 ± 82	247 ± 97	127 ± 47	225 ± 100	138 ± 86
OC	53.3 ± 21.2	69.1 ± 37.4	29.0 ± 14.5	49.9 ± 24.0	23.1 ± 11.5
EC	7.4 ± 1.8	9.6 ± 7.2	3.6 ± 1.7	6.2 ± 2.8	2.5 ± 1.5
WSOC	38.9 ± 14.5	41.5 ± 18.7	21.3 ± 9.3	34.7 ± 14.4	
OC/EC	8.2 ± 2.1	7.8 ± 1.0	7.5 ± 1.9	8.2 ± 2.0	10.0 ± 2.8
WSOC/OC	0.43 ± 0.07	0.45 ± 0.08	0.48 ± 0.13	0.46 ± 0.09	
Na^+	1.0 ± 0.3	1.1 ± 0.3	0.9 ± 0.8	1.2 ± 0.4	1.2 ± 0.6
NH_4	6.6 ± 4.3	7.0 ± 4.1	8.4 ± 3.2	12.4 ± 4.5	1.7 ± 1.1
K^+	4.1 ± 1.6	4.0 ± 2.1	1.3 ± 0.7	2.4 ± 1.0	1.2 ± 0.5
Ca^{2+}	0.9 ± 0.3	2.9 ± 1.4	0.4 ± 0.4	2.0 ± 0.9	3.5 ± 2.2
Cl^-	0.1 ± 0.1	0.3 ± 0.2	0.6 ± 0.6	1.2 ± 0.9	0.6 ± 0.6
NO_3^-	5.1 ± 4.6	5.6 ± 3.1	11.0 ± 5.1	20.6 ± 8.9	4.9 ± 1.6
SO_4^{2-}	20.0 ± 9.6	21.0 ± 11.4	11.4 ± 5.2	19.6 ± 9.2	7.5 ± 2.2

The scattering coefficient (b_{scat}) was measured at 781 nm by a photo-acoustic soot spectrophotometer (PASS; Droplet Measurement Technology, USA).[17] The photomultiplier tube in PASS is configured to measure the scattered optical power using a cosine weighted detector.[18] The instrument was factory calibrated before the experiment and b_{scat} data have a systematic relative uncertainty of 15%.[19] As the wavelength of two measured properties, b_{abs} and b_{scat}, are not identical, an inverse wavelength dependence (λ^{-1}) correction is applied to PASS measured b_{scat} for the estimation of b_{scat} and SSA at 678 nm.[20] The SSA was calculated as the ratio of scattering coefficient to the total extinction coefficient (sum of absorption and scattering coefficients) and all the data with respect to b_{abs}, b_{scat} and SSA are reported at 678 nm in this study. Furthermore, mass scattering efficiency (MSE or σ_{PM10}) is calculated by dividing the scattering coefficient with PM_{10} mass (MSE = b_{scat}/PM_{10}).

The aerosol optical depth was measured at eight spectral channels (340, 380, 440, 500, 670, 870, 940, and 1020 nm)[21−23] using a sun/sky radiometer (CIMEL; spectral range 340−1020 nm) fitted in the Aerosol Robotic Network (AERONET). The uncertainty in calculation of AOD under cloud-free conditions is less than ±0.01 for λ > 440 nm and less than ±0.02 for shorter wavelengths; it is ±10% for retrieval of columnar water-vapor (CWV) and less than ±5% for the sky radiance measurements.[24] The AOD data are provided in three different levels: cloud contaminated (level 1.0) and cloud-screened (level 1.5), following the method described by Smirnov et al.,[25] and quality-assured (level 2.0) has been used in this study.

3. RESULTS AND DISCUSSION

3.1. Mass Concentrations of Carbonaceous Species (OC, EC, and WSOC). The temporal variability in the mass concentrations of OC, EC, and WSOC in $PM_{2.5}$ and PM_{10} is presented in Figure 1. In fine-mode ($PM_{2.5}$), OC concentration varied from 8.9 to 55.7 $\mu gC\ m^{-3}$, and it was systematically higher (13.4 to 90.6 $\mu gC\ m^3$) in PM_{10}. The concentration of EC ranged from 1.0 to 8.8 $\mu gC\ m^{-3}$ (Av: 4.1 ± 2.0 $\mu gC\ m^{-3}$) in $PM_{2.5}$ and from 1.3 to 11.2 $\mu gC\ m^{-3}$ (Av: 5.1 ± 2.9 $\mu gC\ m^{-3}$) in PM_{10}. The average ratios of mass concentrations of OC and EC (in $PM_{2.5}$ to that in PM_{10}) are 0.75 and 0.80, respectively, for the entire sampling period. On average, OC and EC contribute nearly 30% and 4.0%, respectively, to $PM_{2.5}$ mass, whereas, their contribution is relatively low (∼21 and 3%, respectively) in PM_{10}.

In general, mass concentrations of OC, EC, and WSOC are higher during October−December and significantly lower in April (Figure 1a, b, and c, respectively). During March−April, OC and EC concentrations are nearly 2−3 times lower than those during October−January. This systematic decrease in concentrations of carbonaceous species is attributed to the varying source strength of emissions from biomass burning vis-à-vis fossil-fuel combustion and boundary layer dynamics.[10] The concentration of water-soluble K^+, an indicator of biomass burning emission, also exhibits a similar abundance pattern and K^+ concentration is nearly 2 times lower during March−April (Table 1). Although mass concentrations of OC and EC exhibit large temporal variability, OC/EC and WSOC/OC ratios are quite similar during different seasons (Table 1).

The OC/EC and K^+/OC ratios have been used to infer emission sources of carbonaceous aerosols. In this study, K^+/OC ratios (average: 0.05 ± 0.03, range: 0.03−0.08) are similar to those reported for the Savannah burning and agricultural waste burning emissions in India and China.[6,26,27] The OC/EC ratios (average: 8.7 ± 2.3, range: 4.9−13.6) are relatively high, suggesting the dominance of biomass and biofuel emissions as compared to lower OC/EC ratios from fossil fuel (coal and vehicular exhausts) emission.[28−30] The scatter plot between OC and EC shows significant linear correlation (R^2 = 0.80 for n = 54, Figure 2a), suggesting their emission from a common source. Nevertheless, relatively high K^+ concentration, OC/EC ratios, and K^+/OC ratios (similar to agricultural-waste burning) suggest overwhelming contribution of carbonaceous aerosols from biomass and biofuel emissions in the Indo-Gangetic Plain.

The mass concentrations of OC and WSOC were significantly higher in PM_{10} compared to those in $PM_{2.5}$ for the samples collected during winter months (Table 1). The average ratios of mass concentrations of OC and WSOC (in $PM_{2.5}$ to that in PM_{10}) are 0.77 and 0.94, respectively for samples collected during postmonsoon (October−November). These observations are similar to and consistent with those obtained during November 2008 at Kanpur.[6] In contrast, the corresponding average ratios are relatively lower (0.60 and 0.61, respectively) for samples collected during winter months (Table 1). It is noteworthy that concentrations of acidic species (especially NO_3^-) are relatively higher during winter months. Furthermore, the neutralization factor for ammonia

dx.doi.org/10.1021/es202857w | Environ. Sci. Technol. 2012, 46, 686−695

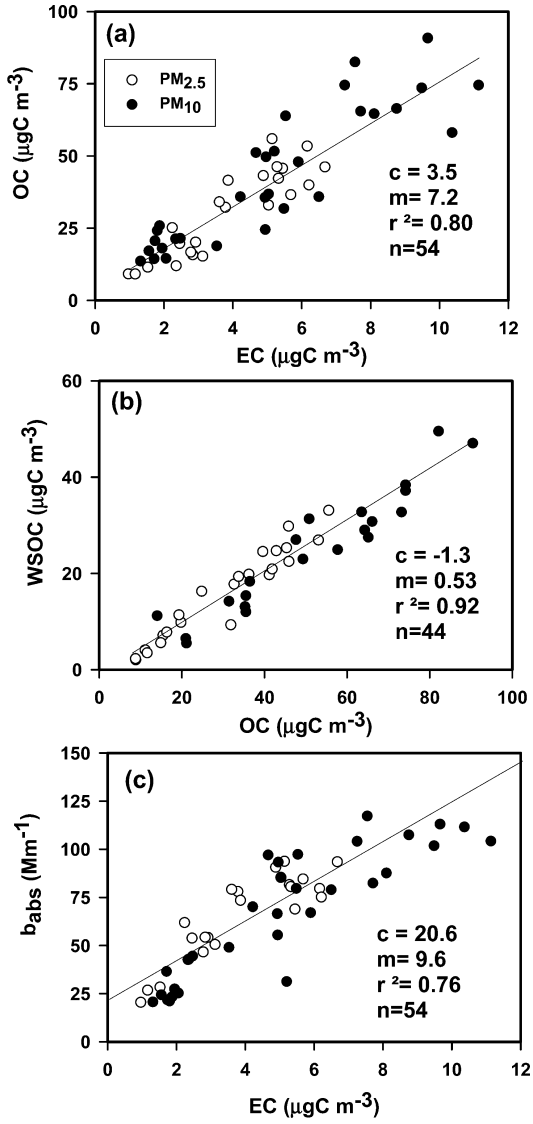

Figure 2. Scatter plots between (a) OC and EC, (b) WSOC and OC, and (c) absorption coefficient (b_{abs}) and EC at Kanpur during Oct 2008–Apr 2009. "m" and "c" are, respectively, the slope and intercept of the best-fit-lines drawn through the data.

(NF; defined as the ratios of equivalent concentrations of NH_4^+ to the sum of SO_4^{2-} and NO_3^-) is much higher during wintertime (NF = 1.12 and 0.94 for $PM_{2.5}$ and PM_{10}, respectively) compared to postmonsoon (NF = 0.73 and 0.74 for $PM_{2.5}$ and PM_{10}, respectively). These observations suggest that fine-mode aerosols, especially those collected during wintertime, are more acidic than PM_{10} samples. The presence of high levels of SO_4^{2-} and NO_3^- results in more acidity to aerosols and thus, preferentially partitions weak organic acids and/or WSOC into coarse-mode aerosols.

3.2. WSOC/OC Ratio and Secondary Formation. As discussed in the previous section, OC/EC ratios are significantly different for biomass burning and fossil fuel emissions. However, OC/EC ratios can also be influenced by the secondary organic aerosol (SOA) formation via the oxidation of volatile organic reactive gases in the atmosphere. It has been proposed that most of the secondary organic products contain polar functional groups. However, SOA formation does not produce refractory EC and, thus, leads to increase in OC/EC and WSOC/OC ratios. WSOC/OC ratios in atmospheric aerosols have been used to infer the extent of secondary aerosol formation and/or aging of aerosols during long-range transport to remote locations.[12,31] The scatter plot between WSOC and OC in $PM_{2.5}$ and PM_{10} shows significant linear relationship (R^2 = 0.92, n = 44, Figure 2b) suggesting that both these constituents are derived from the same primary emission source and/or are influenced by similar secondary processes in the atmosphere.

The WSOC/OC ratios ranged from 0.21 to 0.65 with an average of 0.47 ± 0.11 (for n = 44, figure not shown). A large spread in WSOC/OC ratios further suggests temporal variability in emission sources, their strength, and contribution from SOA at the urban sampling site. WSOC/OC ratios for vehicular emissions are generally low compared to those from biomass burning emissions. The poor solubility of organic constituents from combustion of liquid fuels (diesel, gasoline, etc.) in water is the main reason for lower WSOC/OC ratios. Saarikoski et al.[29] have reported a value of 0.27 for vehicular emissions over an urban environment in Helsinki (northern Europe). An earlier study by Cheung et al.[32] had reported that WSOC/OC ratios vary from 0.06 to 0.19 in the diesel particles emitted from light-duty vehicles. In this context, there is lack of data on WSOC/OC ratios in biomass burning plumes and from direct vehicular/fossil fuel emissions over the Indian region. A recent study from an urban site (Delhi),[33] influenced by vehicular emissions, has reported relatively low WSOC/OC ratios. Mayol-Bracero et al.[34] had reported that WSOC/OC ratios ranged from 0.40 to 0.45 in aerosols collected during the peak of biomass burning season in the Brazilian Amazon region. However, WSOC/OC ratios are relatively low (~0.30–0.40) in aerosols collected during the wintertime over urban atmosphere in northern India when biomass burning emissions are most dominant.[14] The formation of SOAs in the Gangetic Plain during summertime (high photochemical activity) has been suggested by earlier studies.[6,33] For example, Pavuluri et al.[35] have reported that total diacids contributed ~4.0 to 11.0% (average: 6.9%) of WSOC concentrations, arising due to the photochemical formation of water-soluble organic aerosols, at a coastal site (Chennai) in India. We, thus, argue in favor of contribution from SOAs, in addition to primary biomass burning emission, for the enhanced WSOC/OC ratios reported in this study.

3.3. Aerosol Chemical Composition. The $PM_{2.5}$ and PM_{10} mass concentrations range from 32.7 to 189.4 $\mu g\ m^{-3}$ (average: 105.4 ± 45.8 $\mu g\ m^{-3}$, n = 23) and 68.0 to 352.0 $\mu g\ m^{-3}$ (average: 194.9 ± 98.0 $\mu g\ m^{-3}$, n = 31), respectively, during the sampling period. The average $PM_{2.5}$ and PM_{10} mass is relatively higher during postmonsoon (October–November) and winter (December–January) compared to that during summer (March–April) (Table 1). The average mass fraction of carbonaceous and inorganic species in PM_{10} is presented in Figure S1 (Supporting Information). It is noteworthy that contribution of organic matter (OM = 1.6 × OC, where 1.6 is the conversion factor) is maximum among the measured chemical species followed by SO_4^{2-}, NO_3^-, and NH_4^+ during winter and postmonsoon (Figure S1). The mass fraction of OM varies from 33 to 61% in $PM_{2.5}$, whereas it varies from 15 to 54% in PM_{10}. The conversion factor of 1.6 is used to account for the elements other than carbon present in aerosols and ranges from 1.4 to 2.2 depending on the sampling location (urban, rural, or high altitude).[36] A factor of 1.6 is commonly used for converting measured OC to OM in urban

dx.doi.org/10.1021/es202857w | Environ. Sci. Technol. 2012, 46, 686–695

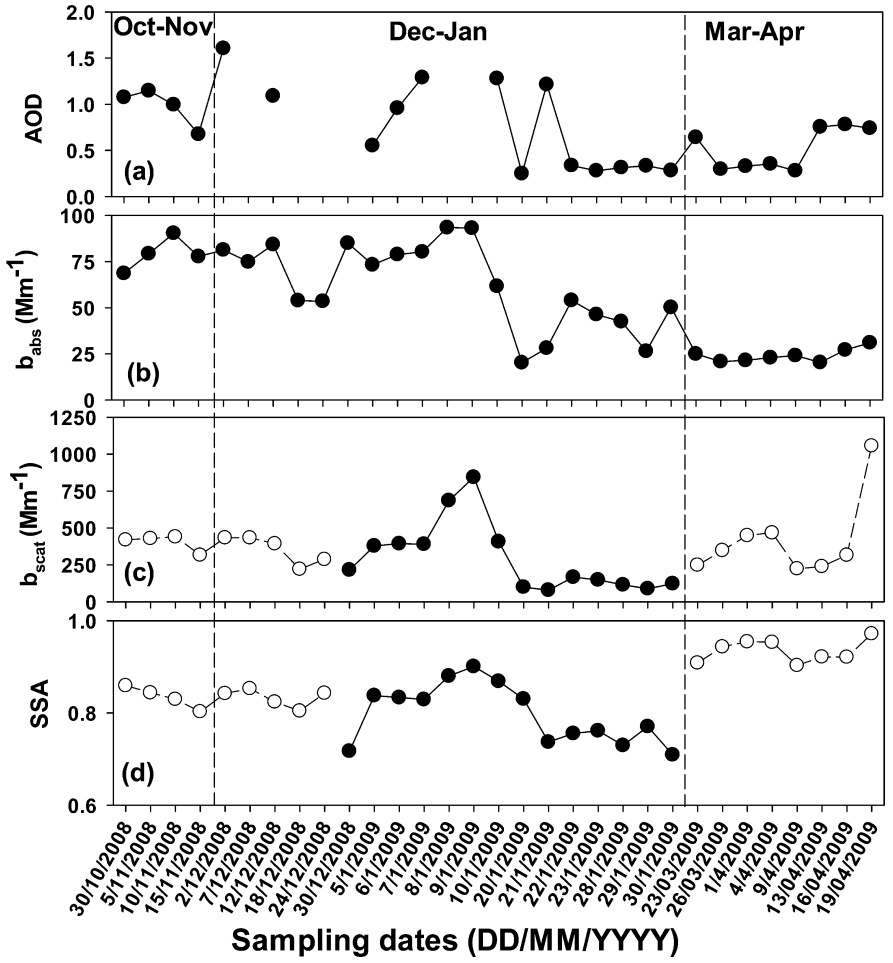

Figure 3. Temporal variation in PM_{10} optical properties. (a) Aerosol optical depth (@500 nm), (b) absorption coefficient (b_{abs}), (c) scattering coefficient (b_{scat}), and (d) single scattering albedo (SSA) during the sampling period (Oct 2008–Apr 2009). The open circles indicate that data for scattering coefficient and SSA were extrapolated using a value of 3.0 m^2 g^{-1} for the mass scattering efficiency and all values are presented at 678 nm wavelength.

atmosphere.[5,10,36] The absorbing EC is a minor constituent of particulate matter and its contribution varied from 1.3 to 7.6% in $PM_{2.5}$ and from 0.9 to 4.8% in PM_{10}.

Secondary inorganic aerosols (SIA, sum of mass concentrations of NH_4^+, NO_3^-, and SO_4^{2-}) contribute ~70–80% of the water-soluble inorganic species (WSIS, sum of mass concentrations of cations and anions) and ~15–25% to the total aerosol mass. The maximum contribution of SIA is seen during the wintertime (~25% in December) and the lowest in April (~10%). Among secondary inorganic species, concentration and mass fraction of SO_4^{2-} is the highest, followed by that of NO_3^- and NH_4^+. The mass fractions of SIAs also decrease gradually after February, a trend quite similar to that observed for carbonaceous species. In contrast, the contribution from unidentified matter (UM) exhibits an increasing trend after January and a maximum (~65% of total mass) was observed in April (Figure S1) when transport of mineral dust is observed over IGP.[10] The concentration of water-soluble Ca^{2+} is used as an indicator of mineral dust.[37,38] The mass concentration of Ca^{2+} increases during March–April, and the highest concentration of Ca^{2+} (9.1 μg m^{-3}) is recorded during a dust storm event on April 19, 2009. These results indicate that transport of mineral dust has a great impact on aerosol chemical composition at Kanpur during summer. The influence of dust storm on changes in optical properties of aerosols is discussed in the subsequent section.

4. OPTICAL PROPERTIES

4.1. Aerosol Absorption Coefficient and Mass Absorption Efficiency. Absorption coefficient is an important parameter to assess the single scattering albedo and direct radiative forcing due to aerosols. The absorption coefficient (b_{abs} at 678 nm) at the study site (Kanpur) also exhibits large temporal variability, quite similar to the temporal trend seen in the concentration of EC. Aerosol absorption coefficient varied from 20 Mm^{-1} (in April; 1 Mm^{-1} = 10^{-6} m^{-1}) to 90 Mm^{-1} in December (Figure 3b). In addition, absorption coefficient shows a significant linear relationship with EC concentration (R^2 = 0.76 for n = 54, Figure 2c), suggesting EC as a major absorbing species of ambient aerosols. However, a nonzero intercept of 20 Mm^{-1} suggests contribution from other absorbing species. A similar linear dependence of b_{abs} on EC concentration has been reported from the field-campaign experiment (PRIDE-PRD 2004) conducted over urban regions in China.[1,39] Using Mie calculation and chemical apportionment, Cheng et al.[39] have suggested that more than 90% of total absorption can be attributed to EC; whereas, Andreae et al.[1] have suggested that nearly 20% of total absorption can arise due to OC and/or internal mixing of aerosols.

dx.doi.org/10.1021/es202857w | Environ. Sci. Technol. 2012, 46, 686–695

Table 2. Seasonally Average Optical Properties of Aerosols at Kanpur during the Sampling Period and Comparison with Other Studies

sites	sampling period	$b_{abs\text{-}678\ nm}(Mm^{-1})$	$b_{scat\text{-}678\ nm}(Mm^{-1})$	SSA	MSE($m^2\ g^{-1}$)	AOD	reference
Kanpur	Oct–Nov 08	79.0 ± 8.9	401.0 ± 57.0[a]	0.83 ± 0.02[a]		1.0 ± 0.2	this study
Kanpur	Dec 08–Jan 09	62.1 ± 22.8	295.0 ± 236.3	0.80 ± 0.06	3.0 ± 0.9	0.8 ± 0.5	this study
Kanpur	Mar–Apr, 2009	24.1 ± 3.6	418.1 ± 273.8[a]	0.93 ± 0.02[a]		0.5 ± 0.2	this study
Delhi	Apr–Jun	62.5 ± 22.3	110.5 ± 36.1	0.63 ± 0.06			Soni et al.[53]
Delhi	Jan–Mar	189.0 ± 86.0	565.6 ± 274.6	0.74 ± 0.03			Soni et al.[53]
China	Mar–Apr, 2009	43 ± 27	379 ± 251	0.87 ± 0.05			Ma et al.[20]
Linan, China	Oct–Dec 1999	23 ± 14	353 ± 202	0.93 ± 0.04			Xu et al.[54]
Beijing, China	Jun 1999	83 ± 40	488 ± 370	0.81 ± 0.08	3.4		Bergin et al.[55]
Gosan	Apr 2001	22 ± 11	240 ± 64	0.91 ± 0.03	2.2 ± 0.1		Kim et al.[56]
Gosan	Nov 2001	25 ± 13	244 ± 123	0.88 ± 0.02	4.5 ± 1.3		Kim et al.[56]
Urban, Atlanta	1999	16 ± 12	121 ± 48	0.87 ± 0.08	3.5–4.4		Carrico et al.[57]
Beijing, PKU	Jan 2005–Dec 2006	56 ± 49	288 ± 281	0.80 ± 0.09			He et al.[58]
Beijing, rural	Aug–Sep 2006	51.8 ± 36.5	361 ± 295	0.86 ± 0.07			Garland et al.[2]
Beijing, SDZ	Sep 03–Jan 05	17.5 ± 13.4	174.6 ± 189.1	0.88			Yan et al.[59]

[a]Estimated using an average mass scattering efficiency (MSE) of 3.0 $m^2\ g^{-1}$ for PM_{10} samples.

Based on OC/EC, K^+/OC ratios, and radiocarbon (^{14}C) analysis of aerosol samples, it has been suggested that biomass burning emissions dominate carbonaceous aerosols loading over Indian region.[5−7,10] Biomass burning emits a significant fraction of humic-like substance (HULIS) and brown carbon.[40−42] Thus, a weak absorbing nature of these compounds can contribute to the measured absorption.[1,40,43] Andreae et al.[1] have derived a value of 0.76 m^2g^{-1} for the specific absorption of OC in Guangzhou aerosols using two-parameter linear regression fit between b_{abs} and carbonaceous species (OC and EC). Assuming this value for the specific absorption of OC, the contribution from OC (to the total absorption) ranges from 20 to 50% in $PM_{2.5}$ and 30 to 90% in PM_{10}. Such high contribution from OC seems unrealistic and unexpected, and arises mainly due to high concentrations of OC (20−30 $\mu g\ m^{-3}$) in these samples. The presence of hematite (Fe_2O_3) in mineral aerosols, with relatively weak absorption characteristic,[44] could also contribute to the measured absorption. Since strength of biomass burning emission decreases significantly during summer, inferred based on a decrease in mass concentration and fractional contribution of OC and EC to total mass, and that of mineral dust increases, thus, relatively higher contribution (to total absorption) is expected from hematite during summer. However, the quantification of absorption from brown carbon, HULIS, and hematite needs further investigation for aerosol absorption properties and estimation of direct aerosol radiative forcing on a regional scale.

A linear regression plot between absorption coefficient (b_{abs}) and EC concentration provides a measure of the mass absorbing efficiency (MAE, σ_{abs}) of EC (Figure 2c). The slope of linear regression analysis between b_{abs} and EC yields MAE of 9.6 $m^2\ g^{-1}$ in $PM_{2.5}$ (R^2 = 0.77, n = 23) and 10.1 $m^2\ g^{-1}$ in PM_{10} (R^2 = 0.78, n = 31). Thus, σ_{abs} does not exhibit size-dependent variability, and two values derived for $PM_{2.5}$ and PM_{10} are not statistically different from each other. The σ_{abs} (this study) is similar to the data reported from urban regions in China and AERONET based retrieval for Asian continental aerosols.[45,46] Also, σ_{abs} is in the range of values reported during the PRIDE-PRD 2004 field-campaign experiment conducted in China; for example 7.7 $m^2\ g^{-1}$ (at urban Guangzhou in $PM_{2.5}$)[1]; 7.2 ± 1.0 (for PM_{10}) and 9.3 ± 1.4 $m^2\ g^{-1}$ (for $PM_{1.0}$) at urban Xinken.[39] More recently, Cheng et al.[47] have measured σ_{abs} (at 632 nm) as 8.45 ± 1.71 and 9.41 ± 1.92 $m^2\ g^{-1}$ for aerosols over Bejing during winter and summer, respectively. Since σ_{abs} exhibits inverse wavelength dependence, data reported in this study (at 678 nm) could be ∼20% higher than σ_{abs} at 550 nm. The higher σ_{abs} may arise due to enhancement in the absorption signal with aging of aerosols, SOA formation, and internal mixing of chemical species at high relative humidity (RH). Bond et al.[48] have suggested that absorption can increase by 50% if BC is internally mixed with water-soluble components. Recently, Lack et al.[49] have found ∼50% enhancement in the measured absorption signal at high RH (73%) compared to lower RH (23%). Furthermore, water-soluble components (WSOC, NH_4^+, SO_4^{2-}, and NO_3^-) are relatively abundant during winter compared to summer (Table 1). Therefore, mixing of water-soluble constituents with BC (i.e., formation of internal mixing) could be highly favored during the wintertime. Our results are, thus, useful for gaining insight into chemical processing and enhanced absorption property of aerosols in the Indo-Gangetic Plain.

4.2. Aerosol Scattering Coefficient, Single Scattering Albedo, and Mass Scattering Efficiency. Aerosol scattering coefficient (b_{scat} at 678 nm) varied from 98 to 1056 Mm^{-1} during the sampling period (Figure 3c). Scattering coefficient during October–November and March–April was calculated using an average mass scattering efficiency (MSE) of 3.0 $m^2\ g^{-1}$ for PM_{10}. The MSE was obtained by dividing scattering coefficient with PM_{10} mass for the samples collected during December–January. The single scattering albedo at 678 nm varied from 0.71 to 0.97 (average: 0.85 ± 0.06) during the sampling period (Figure 3d). The higher absorption and scattering coefficient of aerosols collected during the wintertime are associated with lower SSA, suggesting higher absorbing nature of wintertime aerosols. In contrast, relatively low absorption coefficient and SSA is a conspicuous feature seen in samples from March–April (Table 2). These aerosols are less absorbing type compared to those sampled during October–November (average SSA = 0.82 ± 0.04), though scattering coefficient for the two respective seasons is similar (∼400 Mm^{-1}). The absorption and scattering coefficient, SSA and AOD obtained in this study and at different sites in the world are presented in Table 2.

4.3. Influence of Dust Storm on the Chemical Composition and Optical Properties: A Case Study for

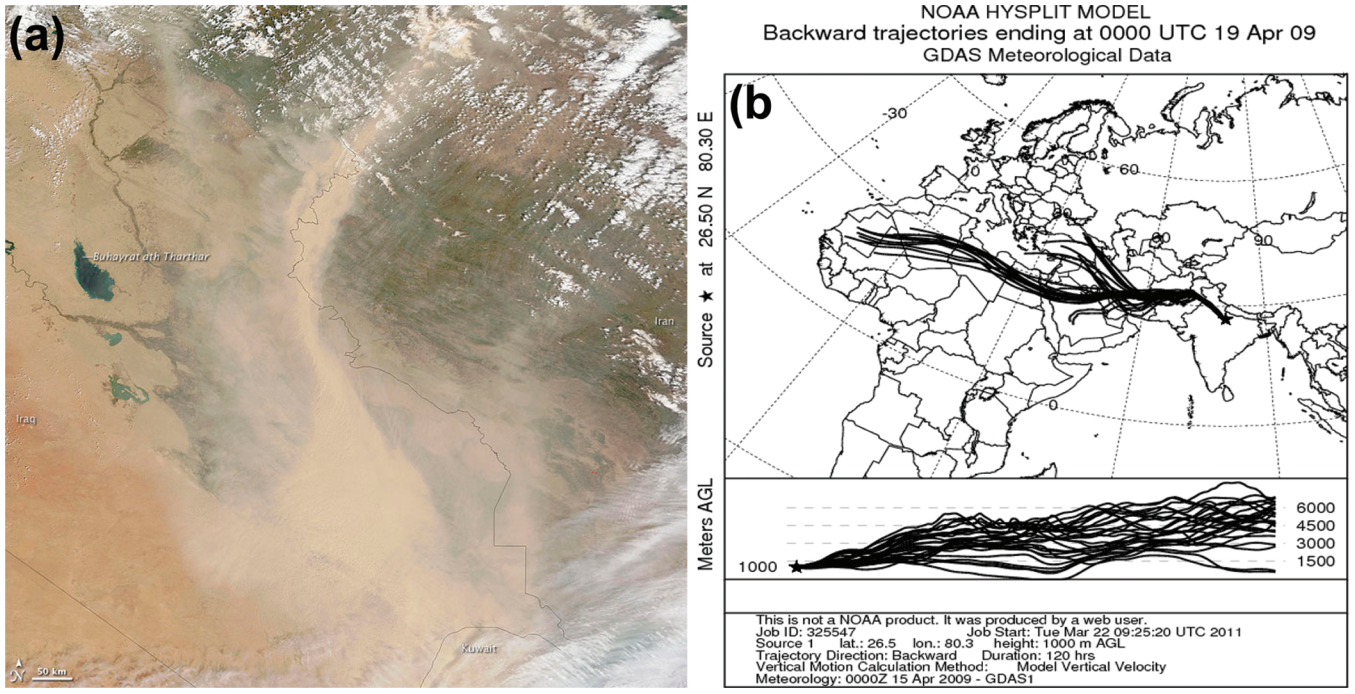

Figure 4. (a) Moderate Resolution Imaging Spectroradiometer (MODIS) on NASA's Aqua satellite picture taken on Apr 15, 2009 showing thick dust plumes over northern Iraq, eastern Syria, and southern Turkey (http://earthobservatory.nasa.gov/NaturalHazards/view.php?id=38228). The MODIS image also captured a dust event on Apr 17, 2009 over the Taklimakan Desert areas of China (figure not shown) which could be associated with the transport of dust originating from Iraq and Turkey. (b) Back-trajectory analysis of air masses arriving at Kanpur on Apr 19, 2009 showing the transport of aerosols from northern Iraq, eastern Syria, and southern Turkey.

April 19, 2009. The occurrence of dust storm events is a common feature in western India, Indo-Gangetic plain, and near the foothills of Himalaya during summer months (March–June). The dust storm events lead to a significant increase in PM_{10} mass (mainly in the coarse mode), aerosol optical depth, and a parallel decrease in the fine-mode mass fraction.[8,50−52] The PM_{10} mass and AOD during the storm event can increase by as much as a factor of 10 depending on the source, wind trajectories, and meteorological parameters (e.g., temperature and wind speed).[52] A thick plume of dust persisted over northern Iraq, eastern Syria, and southern Turkey during mid-April 2009. A Moderate Resolution Imaging Spectroradiometer (MODIS), on NASA's Aqua satellite, picture of dust storm on April 15, 2009 is shown in Figure 4a. Five-day back-trajectory analysis of air-masses arriving at Kanpur (on April 19, 2009) also indicates transport of mineral aerosols from Iraq, Syria, and Turkey through Saudi Arabia, Afghanistan, and Pakistan over India (Figure 4b). The transport of dust proceeded southeast and the MODIS also captured a dust event on April 17, 2009 over the Taklimakan Desert area of China (not shown).

The relative humidity decreased to 20% during the dust storm; whereas, average ambient temperature and wind-speed increased from 16 °C and 0.3 ms^{-1} (in October–January) to 28 °C and 0.6 ms^{-1} in March–April. Under the influence of dust storm, high concentration of PM_{10} mass (352.0 $\mu g\ m^{-3}$) and scattering coefficient (1056 Mm^{-1}) was recorded on April 19, 2009. The mass concentration of Ca^{2+} (used as an index of mineral dust) was also highest (9.1 $\mu g\ m^{-3}$) on 19th April 2009 (2–3 times higher than that during the wintertime). In contrast, mass concentrations of OC and EC were 51.4 and 5.2 $\mu g\ m^{-3}$, respectively; whereas, absorption coefficient decreased to 31.0 Mm^{-1}. Thus, relatively low absorption coefficient and high scattering coefficient led to high SSA of 0.97 during the dust storm (Figure 3d). Furthermore, chemical composition data suggests that mass fractions of carbonaceous aerosols and WSIS decreased to ∼25% and 10%, respectively, and thus, contribution from mineral dust could be as high as 65% (of PM_{10} mass) during the dust event (April 19, 2009).

4.4. Anthropogenic vis-à-vis Natural Aerosols. Based on level 2 data retrieved from AERONET at 500 nm, AODs at Kanpur ranged from 0.25 to 1.61 (average: 0.71 ± 0.41 for n = 25) during the sampling period (Figure 3a). During October–November and December–February period, AODs and $PM_{2.5}/PM_{10}$ ratios are consistently high (Table 2), suggesting the dominance of fine-mode aerosols. Furthermore, chemical composition data indicate that carbonaceous and inorganic aerosols together contribute ∼65–70% of $PM_{2.5}$ mass. In contrast, their contribution is only 40% during March–April (a decrease by ∼50%), and contribution from unidentified matter (largely as mineral dust) is estimated to be ∼60% (Figure S1). Based on the chemical composition of fine- and coarse-mode aerosol fractions, earlier studies have also suggested long-range transport of mineral aerosols to the IGP during summer months.[8,51] The highest mass concentration of PM_{10}, Ca^{2+}, and fractional contribution of unidentified matter (∼65%) is observed on April 19, 2009, when a dust storm event occurred in the Middle East region of Afghanistan and Turkey, indicating transport of mineral dust to the Indo-Gangetic Plain. Thus, the persistent high AODs over IGP are attributed to anthropogenic fine-mode aerosols during the wintertime and that from mineral dust during summer.

The simultaneous measurements comprising chemical composition (carbonaceous and inorganic species) and optical properties (absorption coefficient b_{abs} and mass absorption efficiency σ_{abs}) of ambient aerosols ($PM_{2.5}$ and PM_{10}) has provided important information on the temporal variability in

the abundances of organic matter and mineral dust over an urban site (Kanpur) in the Indo-Gangetic Plain. Aerosol chemical composition data suggest the dominance of organic matter and water-soluble inorganic species during winter months and relative decrease in their contribution and an increase in the abundance of mineral dust during March–April. The high absorption coefficient and low SSA during the wintertime suggest the presence of more absorbing type of aerosols compared to those in the summer. Thus, the long-range transport of mineral aerosols (during summer) and biomass burning emissions (in winter) appear to dominate the chemical composition and optical properties of aerosols in the IGP.

Aerosol absorption coefficient (at 678 nm) and EC concentration are 3–4 times higher during October–January compared to that in March–April. Aerosol absorption is mainly attributed to EC and an average value of 9.6 $m^2\ g^{-1}$ is obtained for mass absorption efficiency at Kanpur. Relatively high mass concentrations of WSOC, SO_4^{2-}, and NO_3^- are observed during the wintertime. These constituents are hygroscopic in nature and, thus, can contribute significantly to the total scattering coefficient via hygroscopic growth of aerosols. Furthermore, aging and secondary aerosol formation are important processes contributing to enhancement in the absorption signal by forming internal mixture of aerosols at high relative humidity in the IGP. These findings have implications to severe fog-haze weather conditions, a seasonal feature, in the Indo-Gangetic Plain during the wintertime.

■ ASSOCIATED CONTENT

Supporting Information

Figure S1: stacked column plots for the monthly averaged concentrations of various chemical species in the total aerosol mass (in PM_{10} samples) at Kanpur during measurement period. This material is available free of charge via the Internet at http://pubs.acs.org.

■ AUTHOR INFORMATION

Corresponding Author

*E-mail: sarin@prl.res.in; tel: +91 79 26314306; fax: +91 79 26301502.

Present Address

[‖]Department of Earth and Planetary Science, Graduate School of Science, University of Tokyo, Tokyo, Japan 113-0033.

■ ACKNOWLEDGMENTS

We acknowledge the financial support received from the Indian Space Research Organization-Geosphere Biosphere program office (Bengaluru, India). S.N.T. thanks the PIs for their effort in establishing and maintaining AERONET site at Kanpur. We are thankful to two anonymous reviewers for their constructive comments and suggestions.

■ REFERENCES

(1) Andreae, M. O.; Schmid, O.; Yang, H.; Chand, D.; Yu, J. Z.; Zeng, L.-M.; Zhang, Y.-H. Optical properties and chemical composition of the atmospheric aerosol in urban Guangzhou, China. *Atmos. Environ.* **2008**, *42*, 6335–6350.

(2) Garland, R. M.; Schmid, O.; Nowak, A.; Achtert, P.; Wiedensohler, A.; Gunthe, S. S.; Takegawa, N.; Kita, K.; Kondo, Y.; Hu, M.; Shao, M.; Zeng, L. M.; Zhu, T.; Andreae, M. O.; Pöschl, U. Aerosol optical properties observed during Campaign of Air Quality Research in Beijing 2006 (CAREBeijing-2006): Characteristic differences between the inflow and outflow of Beijing city air. *J. Geophys. Res.* **2009**, *114* (D2), D00G04.

(3) Rengarajan, R.; Sudheer, A. K.; Sarin, M. M. Aerosol acidity and secondary organic aerosol formation during wintertime over urban environment in western India. *Atmos. Environ.* **2011**, *45*, 1940–1945.

(4) Prasad, A. K.; Singh, R. P.; Kafatos, M. Influence of coal based thermal power plants on aerosol optical properties in the Indo-Gangetic basin. *Geophys. Res. Lett.* **2006**, *33*, L05805 DOI: 10.1029/2005GL023801.

(5) Rengarajan, R.; Sarin, M. M.; Sudheer, A. K. Carbonaceous and inorganic species in atmospheric aerosols during wintertime over urban and high-altitude sites in North India. *J. Geophys. Res.* **2007**, *112*, D21307 DOI: 10.1029/2006JD008150.

(6) Ram, K.; Sarin, M. M. Day-night variability of EC, OC, WSOC and inorganic ions in urban environment of Indo-Gangetic Plain: Implications to secondary aerosol formation. *Atmos. Environ.* **2011**, *45*, 460–468.

(7) Gustafsson, Ö.; Kruså, M.; Zencak, Z.; Sheesley, R. J.; Granat, L.; Engström, E.; Praveen, P. S.; Rao, P. S. P.; Leck, C.; Rodhe, H. Brown Clouds over South Asia: Biomass or Fossil Fuel Combustion? *Science* **2009**, *323*, 495–498.

(8) Chinnam, N.; Dey, S.; Tripathi, S. N.; Sharma, M. Dust events in Kanpur, northern India: Chemical evidence for source and implications to radiative forcing. *Geophys. Res. Lett.* **2006**, *33*, L08803 DOI: 10.1029/ 2005GL025278.

(9) Rastogi, N.; Sarin, M. M. Chemistry of aerosols over a semi-arid region: Evidence for acid neutralization by mineral dust. *Geophys. Res. Lett.* **2006**, *33*, L23815 DOI: 10.1029/2006GL027708.

(10) Ram, K.; Sarin, M. M.; Tripathi, S. N. A 1 year record of carbonaceous aerosols from an urban location (Kanpur) in the Indo-Gangetic Plain: Characterization, sources and temporal variability. *J. Geophys. Res.* **2010**, *115*, D24313 DOI: 10.1029/2010JD014188.

(11) Ramanathan, V.; Ramana, M. V. Persistent, widespread, and strongly absorbing haze over the Himalayan foothills and the Indo-Gangetic plains. *Pure Appl. Geophys.* **2005**, *162*, 1609–1626.

(12) Aggarwal, S. G.; Kawamura, K. Carbonaceous and inorganic composition in long-range transported aerosols over northern Japan: Implication for aging of water-soluble organic fraction. *Atmos. Environ.* **2009**, *43* (16), 2532–2540.

(13) Dey, S.; Tripathi, S. N.; Mishra, S. K. Probable mixing state of aerosols in the Indo-Gangetic Basin, northern India. *Geophys. Res. Lett.* **2008**, *35*, L03808 DOI: 10.1029/2007GL032622.

(14) Ram, K.; Sarin, M. M. Spatio-temporal variability in atmospheric abundances of EC, OC and WSOC over northern India. *J. Aerosol Sci.* **2010**, *41* (1), 88–98.

(15) Ram, K.; Sarin, M. M.; Hegde, P. Atmospheric abundances of primary and secondary carbonaceous species at two high-altitude sites in India: Sources and temporal variability. *Atmos. Environ.* **2008**, *42* (28), 6785–6796.

(16) Ram, K.; Sarin, M. M. Absorption coefficient and site-specific mass absorption efficiency of elemental carbon in aerosols from urban, rural, and high-altitude sites in India. *Environ. Sci. Technol.* **2009**, *43*, 8233–8239.

(17) Jai Devi, J.; Tripathi, S. N.; Gupta, T.; Singh, B. N.; Gopalakrishnan, V.; Dey, S. Observation-based 3-D view of aerosol radiative properties over Indian Continental Tropical Convergence Zone: Implications to regional climate. *Tellus B* **2011**, *63* (5), 971–989.

(18) Arnott, W. P.; Moosmuller, H.; Rogers, C. F.; Jin, T.; Bruch, R. Photoacoustic spectrometer for measuring light absorption by aerosol: Instrument description. *Atmos. Environ.* **1999**, *33* (17), 2845–2852.

(19) Lewis, K.; Arnott, W. P.; Moosmüller, H.; Wold, C. E. Strong spectral variation of biomass smoke light absorption and single scattering albedo observed with a novel dual-wavelength photoacoustic instrument. *J. Geophys. Res.* **2008**, *113*, D16203 DOI: 10.1029/2007JD009699.

(20) Ma, N.; Zhao, C. S.; Nowak, A.; Muller, T.; Pfeifer, S.; Cheng, Y. F.; Deng, Z. Z.; Liu, P. F.; Xu, W. Y.; Ran, L.; Yan, P.; Gabel, T.; Hallbauer, E.; Mildenberger, K.; Henning, S.; Yu, J.; Chen, L. L.; Zhou,

X. J.; Stratmann, F.; Wiedensohler, A. Aerosol optical properties in the North China Plain during HaChi campaign: An in-situ optical closure study. *Atmos. Chem. Phys.* **2011**, *11* (12), 5959−5973.
(21) Singh, R. P.; Dey, S.; Tripathi, S. N.; Tare, V.; Holben, B. N. Variability of aerosol parameters over Kanpur, northern India. *J. Geophys. Res.* **2004**, *109*, D23206 DOI: 10.1029/2004JD004966.
(22) Dey, S.; Tripathi, S. N. Aerosol direct radiative effects over Kanpur in the Indo-Gangetic basin, northern India: Long-term (2001−2005) observations and implications to regional climate. *J. Geophys. Res.* **2008**, *113*, D04212 DOI: 10.1029/2007JD009029.
(23) Holben, B. N.; Eck, T. F.; Slutsker, I.; Tanré, D.; Buis, J. P.; Setzer, A.; Vermote, E.; Reagan, J. A.; Kaufman, Y. J.; Nakajima, T.; Lavenu, F.; Jankowiak, I.; Smirnov, A. AERONET-A Federated Instrument Network and Data Archive for Aerosol Characterization. *Remote Sens. Environ.* **1998**, *66* (1), 1−16.
(24) Dubovik, O.; Smirnov, A.; Holben, B. N.; King, M. D.; Kaufman, Y. J.; Eck, T. F.; Slutsker, I. Accuracy assessments of aerosol optical properties retrieved from Aerosol Robotic Network (AERONET) Sun and sky radiance measurements. *J. Geophys. Res.* **2000**, *105* (D8), 9791−9806.
(25) Smirnov, A.; Holben, B. N.; Eck, T. F.; Dubovik, O.; Slutsker, I. Cloud-Screening and Quality Control Algorithms for the AERONET Database. *Remote Sens. Environ.* **2000**, *73* (3), 337−349.
(26) Andreae, M. O. Soot carbon and excess fine potassium: Long-range transport of combustion-derived aerosols. *Science* **1983**, *220* (4602), 1148−1151.
(27) Echalar, F.; Gaudichet, A.; Cachier, H.; Artaxo, P. Aerosol emissions by tropical forest and savanna biomass burning: characteristic trace elements and fluxes. *Geophys. Res. Lett.* **1995**, *22* (22), 3034−3042.
(28) Andreae, M. O.; Merlet, P. Emission of trace gases and aerosols from biomass burning. *Global Biogeochem. Cycles* **2001**, *15* (4), 955−966.
(29) Saarikoski, S.; Timonen, H.; Saarnio, K.; Aurela, M.; Jarvi, L.; Keronen, P.; Kerminen, V.-M.; Hillamo, R. Sources of organic carbon in fine particulate matter in northern European urban air. *Atmos. Chem. Phys.* **2008**, *8*, 6281−6295.
(30) Zhu, C.-S.; Chen, C.-C.; Cao, J.-J.; Tsai, C.-J.; Chou, C. C. K.; Liu, S.-C.; Roam, G.-D. Characterization of carbon fractions for atmospheric fine particles and nanoparticles in a highway tunnel. *Atmos. Environ.* **2010**, *44* (23), 2668−2673.
(31) Zhang, Q.; Jimenez, J. L.; Canagaratna, M. R.; Allan, J. D.; Coe, H.; Ulbrich, I.; Alfarra, M. R.; Takami, A.; Middlebrook, A. M.; Sun, Y. L.; Dzepina, K.; Dunlea, E.; Docherty, K.; DeCarlo, P. F.; Salcedo, D.; Onasch, T.; Jayne, J. T.; Miyoshi, T.; Shimono, A.; Hatakeyama, S.; Takegawa, N.; Kondo, Y.; Schneider, J.; Drewnick, F.; Borrmann, S.; Weimer, S.; Demerjian, K.; Williams, P.; Bower, K.; Bahreini, R.; Cottrell, L.; Griffin, R. J.; Rautiainen, J.; Sun, J. Y.; Zhang, Y. M.; Worsnop, D. R. Ubiquity and dominance of oxygenated species in organic aerosols in anthropogenically-influenced Northern Hemisphere midlatitudes. *Geophys. Res. Lett.* **2007**, *34*, L13801 DOI: 10.1029/2007GL029979.
(32) Cheung, K. L.; Polidori, A.; Ntziachristos, L.; Tzamkiozis, T.; Samaras, Z.; Cassee, F. R.; Gerlofs, M.; Sioutas, C. Chemical Characteristics and Oxidative Potential of Particulate Matter Emissions from Gasoline, Diesel, and Biodiesel Cars. *Environ. Sci. Technol.* **2009**, *43* (16), 6334−6340.
(33) Miyazaki, Y.; Aggarwal, S. G.; Singh, K.; Gupta, P. K.; Kawamura, K. Dicarboxylic acids and water-soluble organic carbon in aerosols in New Delhi, India in winter: Characteristics and formation processes. *J. Geophys. Res.* **2009**, *114*, D19206 DOI: 10.1029/2007JD009116.
(34) Mayol-Bracero, O. L.; Guyon, P.; Roberts, B. G.; Andreae, M. O.; Decesari, S.; Facchini, M. C.; Fuzzi, S.; Artaxo, P. Water-soluble organic compounds in biomass burning aerosols over Amazonia. 2. Apportionment of the chemical composition and importance of the polyacidic fraction. *J. Geophys. Res.* **2002**, *107* (D20), 8047 DOI: 10.1029/2001JD000522.
(35) Pavuluri, C. M.; Kawamura, K.; Swaminathan, T. Water-soluble organic carbon, dicarboxylic acids, ketoacids, and α-dicarbonyls in the tropical Indian aerosols. *J. Geophys. Res.* **2010**, *115*, D11302 DOI: 10.1029/2009JD012661.
(36) Turpin, B. J.; Lim, H.-J. Species contributions to $PM_{2.5}$ mass concentrations: Revisiting common assumptions for estimating organic mass. *Aerosol Sci. Technol.* **2001**, *35* (1), 602−610.
(37) Lin, C.-Y.; Wang, Z.; Chen, W.-N.; Chang, S.-Y.; Chou, C. C. K.; Sugimoto, N.; Zhao, X. Long-range transport of Asian dust and air pollutants to Taiwan: observed evidence and model simulation. *Atmos. Chem. Phys.* **2007**, *7* (2), 423−434.
(38) Putaud, J.-P.; Van Dingenen, R.; Dell' Acqua, A.; Raes, F.; Matta, E.; Decesari, S.; Facchini, M. C.; Fuzzi, S. Size-segregated aerosol mass closure and chemical composition in Monte Cimone (I) during MINATROC. *Atmos. Chem. Phys.* **2004**, *4* (4), 889−902.
(39) Cheng, Y. F.; Wiedensohler, A.; Eichler, H.; Su, H.; Gnauk, T.; Bruggemann, E.; Herrmann, H.; Heintzenber, J.; Slanina, J.; Tuch, T.; Hu, M.; Zhang, Y. H. Aerosol optical properties and related chemical apportionment at Xinken in Pearl River Delta of China. *Atmos. Environ.* **2008**, *42*, 6351−6372.
(40) Andreae, M. O.; Gelencser, A. Black carbon or brown carbon? The nature of light-absorbing carbonaceous aerosols. *Atmos. Chem. Phys.* **2006**, *6* (10), 3131−3148.
(41) Arola, A.; Schuster, G.; Myhre, G.; Kazadzis, S.; Dey, S.; Tripathi, S. N. Inferring absorbing organic carbon content from AERONET data. *Atmos. Chem. Phys.* **2011**, *11* (1), 215−225.
(42) Lary, D.; Lee, A.; Toumi, R.; Newchurch, M.; Pirre, M.; Renard, J. Carbon aerosols and atmospheric photochemistry. *J. Geophys. Res.* **1997**, *102* (D3), 3671−3682.
(43) Kirchstetter, T. W.; Novakov, T.; Hobbs, P. V. Evidence that the spectral dependence of light absorption by aerosols is affected by organic carbon. *J. Geophys. Res.* **2004**, *109*, D21208 DOI: 10.1029/2004JD004999.
(44) Bodhaine, B. A. Aerosol absorption measurements at Barrow, Mauna Loa and the south pole. *J. Geophys. Res.* **1995**, *100* (D5), 8967−8975.
(45) Schuster, G. L.; Dubovik, O.; Holben, B. N.; Clothiaux, E. E. Inferring black carbon content and specific absorption from Aerosol Robotic Network (AERONET) aerosol retrievals. *J. Geophys. Res.* **2005**, *110*, D10S17 DOI: 10.1029/2004JD004548.
(46) Dey, S.; Tripathi, S. N. Retrieval of black carbon and specific absorption over Kanpur city, northern India during 2001−2003 using AERONET data. *Atmos. Environ.* **2006**, *40*, 445−456.
(47) Cheng, Y.; He, K. B.; Zheng, M.; Duan, F. K.; Du, Z. Y.; Ma, Y. L.; Tan, J. H.; Yang, F. M.; Liu, J. M.; Zhang, X. L.; Weber, R. J.; Bergin, M. H.; Russell, A. G. Mass absorption efficiency of elemental carbon and water-soluble organic carbon in Beijing, China. *Atmos. Chem. Phys.* **2011**, *11* (22), 11497−11510.
(48) Bond, T. C.; Habib, G.; Bergstrom, R. W. Limitations in the enhancement of visible light absorption due to mixing state. *J. Geophys. Res.* **2006**, *111*, D20211 DOI: 10.1029/2006JD007315.
(49) Lack, D. A.; Quinn, P. K.; Massoli, P.; Bates, T. S.; Coffman, D.; Covert, D. S.; Sierau, B.; Tucker, S.; Baynard, T.; Lovejoy, E.; Murphy, D. M.; Ravishankara, A. R. Relative humidity dependence of light absorption by mineral dust after long-range atmospheric transport from the Sahara. *Geophys. Res. Lett.* **2009**, *36* (24), L24805.
(50) Ram, K.; Sarin, M. M.; Hegde, P. Long-term record of aerosol optical properties and chemical composition from a high-altitude site (Manora Peak) in Central Himalaya. *Atmos. Chem. Phys.* **2010**, *10* (23), 11791−11803.
(51) Jethva, H.; Satheesh, S. K.; Srinivasan, J. Seasonal variability of aerosols over the Indo-Gangetic basin. *J. Geophys. Res.* **2005**, *110*, D21204 DOI: .1029/2005JD005938.
(52) Hegde, P.; Pant, P.; Naja, M.; Dumka, U. C.; Sagar, R. South Asian dust episode in June 2006: Aerosol observations in the central Himalayas. *Geophys. Res. Lett.* **2007**, *34*, L23802 DOI: 10.1029/2007GL030692.
(53) Soni, K.; Singh, S.; Bano, T.; Tanwar, R. S.; Nath, S.; Arya, B. C. Variations in single scattering albedo and Angstrom absorption

exponent during different seasons at Delhi, India. *Atmos. Environ.* **2010**, *44* (35), 4355−4363.
(54) Xu, J.; Bergin, M. H.; Yu, X.; Liu, G.; Zhao, J.; Carrico, C. M.; Baumann, K. Measurement of aerosol chemical, physical and radiative properties in the Yangtze delta region of China. *Atmos. Environ.* **2002**, *36* (2), 161−173.
(55) Bergin, M. H.; Cass, G. R.; Xu, J.; Fang, C.; Zeng, L. M.; Yu, T.; Salmon, L. G.; Kiang, C. S.; Tang, X. Y.; Zhang, Y. H.; Chameides, W. L. Aerosol radiative, physical, and chemical properties in Beijing during June 1999. *J. Geophys. Res.* **2001**, *106* (D16), 17969−17980.
(56) Kim, S.-W.; Yoon, S.-C.; Jefferson, A.; Ogren, J. A.; Dutton, E. G.; Won, J.-G.; Ghim, Y. S.; Lee, B.-I.; Han, J.-S. Aerosol optical, chemical and physical properties at Gosan, Korea during Asian dust and pollution episodes in 2001. *Atmos. Environ.* **2005**, *39* (1), 39−50.
(57) Carrico, C. M.; Bergin, M. H.; Xu, J.; Baumann, K.; Maring, H. Urban aerosol radiative properties: Measurements during the 1999 Atlanta Supersite Experiment. *J. Geophys. Res.* **2003**, *108* (D7), 8422 DOI: 10.1029/2001JD001222.
(58) He, X.; Li, C. C.; Lau, A. K. H.; Deng, Z. Z.; Mao, J. T.; Wang, M. H.; Liu, X. Y. An intensive study of aerosol optical properties in Beijing urban area. *Atmos. Chem. Phys.* **2009**, *9* (22), 8903−8915.
(59) Yan, P.; Tang, J.; Huang, J.; Mao, J. T.; Zhou, X. J.; Liu, Q.; Wang, Z. F.; Zhou, H. G. The measurement of aerosol optical properties at a rural site in Northern China. *Atmos. Chem. Phys.* **2008**, *8*, 2229−2242.